A study on the structure and precipitation processes of precipitating stratiform clouds associated with a westerly trough

Tuanjie Hou, Hengchi Lei, Zhaoxia Hu
Institute of Atmospheric Physics, Chinese Academy of Sciences, Beijing, China 100029

1. Introduction

Formation of precipitation in stratiform clouds is quite complicated due to differences in updraft, liquid water content and ice particle growth modes, and so on. A series of aircraft observations and numerical simulations (Hobbs et al., 1975; Herzegh and Hobbs, 1980; Lo and Passarelli, 1982; Field, 1999; Field and Heymsfield, 2003; Heymsfield et al., 2008) of precipitation processes in frontal clouds and midlatitude cyclones have been conducted since the 1970s. In Apr 2009, three-aircraft simultaneous observations of different levels for the same cloud were first conducted in China, providing important data for the research of stratiform cloud precipitation. Based on airborne cloud particle probe observations, Doppler radar measurements and surface precipitation data, the cloud structure and precipitation processes were studied comprehensively with the Weather Research and Forecasting (WRF) model.

2. Observations

2.1. Observational facilities

During Apr and May 2009, three research aircraft, X-band radar, tilting bucket rain gauges and rawinsondes were utilized to provide various information of target clouds. The airborne observational data were obtained from probes mounted on three aircraft, including Forward Scattering Spectrometer Probe (FSSP-100), Optical Array Prove 2D-C and 2D-P on Xiayan ⅢA of Hebei Province, Cloud Droplet Probe (CDP), Cloud Imaging Probe (CIP) and Precipitation Imaging Probe (PIP) on Y-12E of Shanxi Province, and Cloud and Aerosol Spectrometer (CAS), CIP and PIP on Y-12E of Beijing City.

2.2. Synoptic settings and precipitation

Affected by a westerly trough and cold front, moderate precipitation occurred over Northern Hebei Province of China from 30 Apr to 1 May 2009.

The 30-h precipitation during 08 LT (Beijing local time) on 30 Apr and 14 on 1 May obtained from rain gauges is displayed in Fig. 1. According to Fig. 1, light rain with total rainfall of less than 10 mm was recorded at most stations and moderate rain with the maximum value of 14 mm was recorded at some stations.

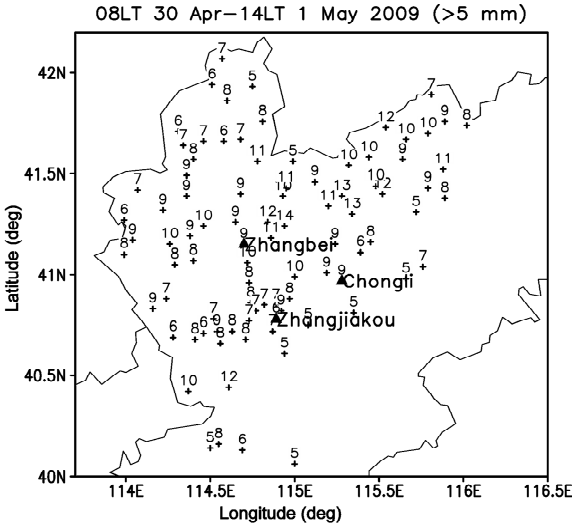

Fig. 1 The observed 30-h precipitation during 08 on 30 Apr and 14 on 1 May 2009

Fig. 2 shows the distribution of relative humidity with height at four selected times from 20 LT on 30 Apr to 08 LT on 1 May.

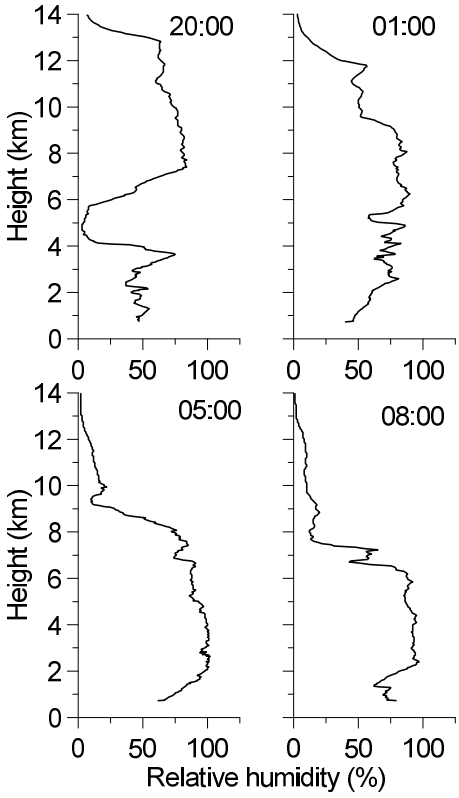

Fig. 2 Distribution of relative humidity with height from 20 LT on 30 Apr to 08 LT on 1 May

Fig. 2 suggests that at 20 LT on 30 Apr, the air at high levels 7.1-10.5 km was rather moist, with a relative humidity of over 70 %, but it became dry rapidly at around 5 km, indicating cloud formation process starting with the appearance of high-level clouds. By 01 LT on 1 May, the relative humidity at all levels between 1.2 and 10.0 km had been over 50 %, suggesting development of updraft from the lower levels. At 05 LT, the relative humidity between 1.2 and 7.6 km increased to over 80 % and even to 100 % or 101 % at 2.0-4.0 km, suggesting the existence of clouds in that region. At 08 LT, the RH with the value of 80 % only existed below 6.3 km, which indicated dissipation of high-level clouds and precipitation of middle and lower clouds.

The X-band radar located at Zhangbei provides information of cloud development. Radar images indicated that the clouds were characterized by the horizontal extension of 100-200 km, reflectivity values of 35-40 dBZ and echo top of over 6.0 km at the mature stage. After 08 LT on 1 May, reflectivity values decreased to 20-35 dBZ at most regions.

2.3. Micro-scale features of clouds

Aircraft observations were conducted at the time of the late mature stage changing to the decaying stage, during 08:20 LT and 11:20 LT on 1 May. Average liquid water content (LWC) at different levels measured by 1D droplet probes is listed in Table 1. Table 1 indicates that average values of LWC at 4.8, 5.4 and 6.0 km were very small, with the magnitude of 0.001 g m^{-3}, which suggests the dissipation of clouds from higher levels. It is worth noting that, for 3.6 km, the average LWC values were 0.04 and 0.05 g m^{-3} before 09:56, but decreased rapidly to only 0.001 g m^{-3} during 10:02—10:12. It suggests that dissipation of lower clouds was also quite obvious.

Table 1 Average LWC for every 10 min at different levels

Time (hh:mm)	Height (km)	Average LWC (g m^{-3})
	4.8	0.007
	4.2	0.001
09:30—09:40	3.6	0.037
	5.4	0.002
	4.2	0.015
09:46—09:56	3.6	0.053
	6.0	0.003
	4.2	0.003
10:02—10:12	3.6	0.001

Fig. 3 shows the evolution of cloud particles during 09:30 and 10:15 measured by the 2D cloud probes. According to Fig. 3, low cloud particle concentration of less than 5 L^{-1} was observed at levels 4.8-6.0 km, while high concentration of up to 10^2 L^{-1} occurred at 3.6 and 4.2 km. In addition, cloud particle concentration varied little at 4.2 km but decreased evidently at 3.6 km

after 10:00. The results suggested that ice particle grew actively at 3.6 and 4.2 km, but later weakened at both higher and lower parts.

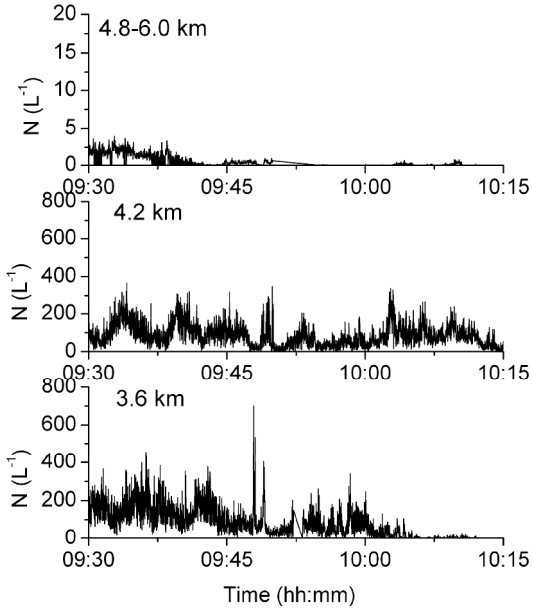

Fig. 3 The evolution of cloud particles during 09:30 and 10:15 measured by the 2D cloud probes

For further understanding of cloud structure and precipitation processes at various stages, the WRF model was used to simulate the cloud development.

3. Numerical simulation

3.1. Model setup

The model configuration consisted of a nested two-way nested domain defined on a Lambert conformal projection. A 4-km grid model (domain 2, 76×76) covering northeastern Hebei Province was surrounded by 12-km model (domain 1, 74×74) by a two-way nesting interaction (Fig. 4). The number of vertical levels was 37. The 1-degree GRIB1 data download from NCEP was used to initialize the model. The physical packages include RRTM longwave radiation scheme, Dudhia shortwave radiation scheme, Monin-Obukhov based surface layer scheme, Noah land surface model, the Yonsei University planetary boundary layer and Morrison double-moment scheme were considered in both domains. The difference between the two domains was that Kain-Fritsch cumulus parameterization scheme was turned off in domain 2. The model was integrated for 30 h from 08 LT on 30 Apr to 14 LT on 1 May 2009 with a time step of 60 s for domain 1 and for 18 h from 20 LT on 30 Apr to 14 LT on 1 May 2009 with a time step of 20 s for domain 2.

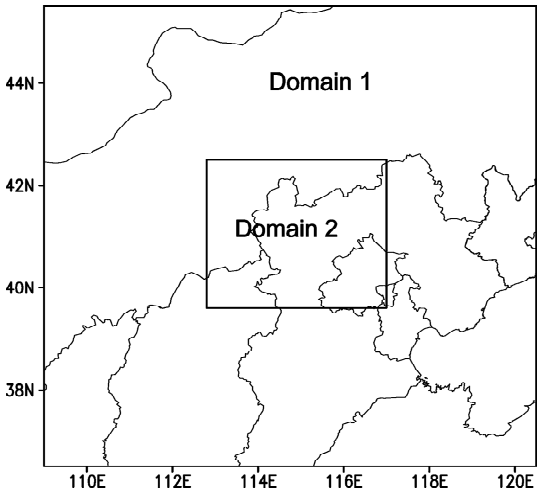

Fig. 4 Model domains

On the whole, the model was quite successful in simulating the major rainfall region and the movement of the rainband, with better results at the mature stage than the dissipating stage of precipitation. The simulated accumulated precipitation was a little smaller than that from observation, but still could be used to analyze the microphysical processes and corresponding precipitation mechanisms.

3.2. Results

Updraft is an important parameter to reflect the development intensity of clouds. Hence, Fig. 5 displays height-longitude cross sections of updrafts while latitude is 41^{o} N at 04 LT and 06 LT on 1 May.

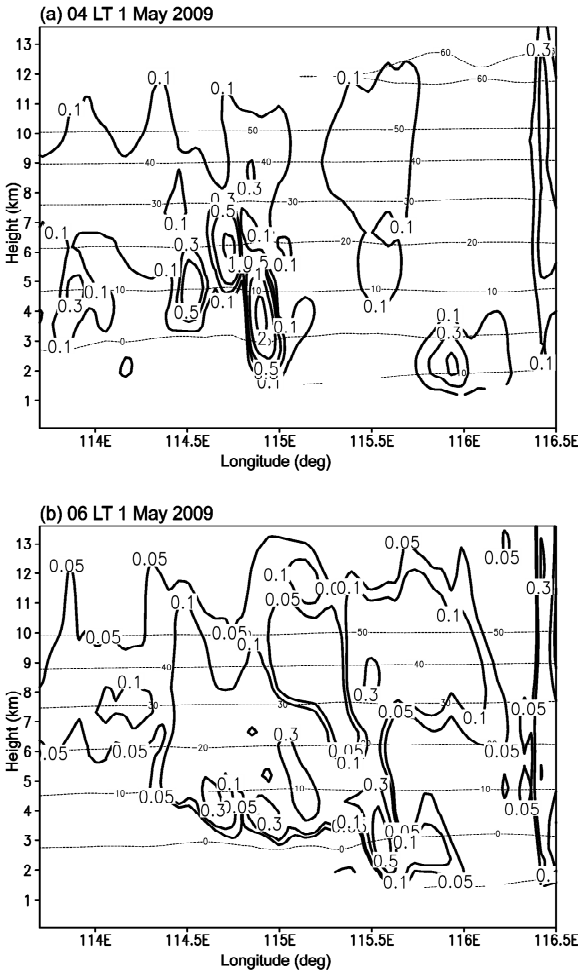

Fig. 5 Height-longitude cross sections of updrafts while latitude is 41° N at 04 LT and 06 LT on 1 May

At 04 LT (Fig. 5a), the updraft center developed to the height of 4.0 km, with the maximum value of up to 2.0 m s^{-1} at 115°E. It indicated the presence of embedded convective cells in the stratiform clouds. After that, the clouds moved towards northeast and became weaker. By 06 LT (Fig. 5b), those updraft center values had decreased to 0.3-0.5 m s^{-1}.

Taking Zhangbei station as an example, Fig. 6 displays vertical distributions of updrafts and hydrometers at selected times.

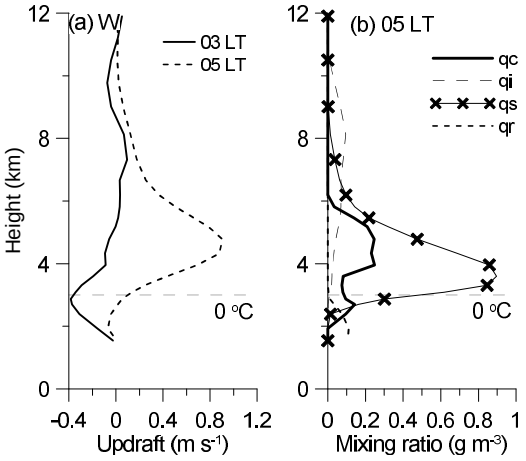

Fig. 6 Vertical distributions of updrafts at 03 LT and 05 LT, and hydrometers at 05 LT. qc-cloud water; qi-cloud ice; qs- snow; qr- rain

According to Fig. 6 (a), updraft were negative below 5 km at 03 LT, suggesting start of upward development. By 05 LT, the maximum updraft had increased to 0.9 m s^{-1}, located at 4.8 km. That suggested that the cloud developed rather strongly, not just uniform stratiform cloud. Fig. 5 (b) shows that the maximum value of cloud water was 0.25 g m^{-3} due to condensation and the top height was at 6.2 km. At that time, snow was the main precipitation particles with the maximum value of up to 0.9 g m^{-3}, at levels above the 0°C layer. High values of snow corresponded to low value of cloud water, suggesting riming of snow by consuming cloud water. In addition, the content of rain was also increased to 0.11 g m^{-3}, so relatively high precipitation rates were observed at that stage.

As the main precipitation particles in the mixed phase region, growth modes of snow greatly affect the formation and intensity of precipitation. Therefore, Fig. 7 displays the percentages of four main growth modes accounted for the total mass source at 05 LT.

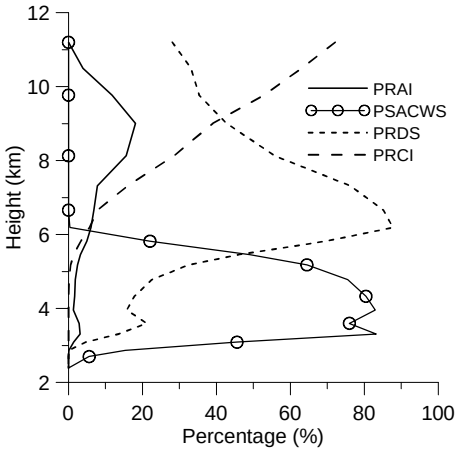

Fig. 7 Percentages of four main growth modes accounted for the total mass source at 05 LT. PRAI—autoconversion of cloud ice to snow, PSACWS—droplet accretion of snow; PRDS—depositional growth of snow; PRCI—ice accretion of snow

Fig. 7 shows that snow formed initially from autoconversion of cloud ice at the upper part, which accounted for about 60 % of total mass source and became less important with the decrease of height. Ice accretion of snow accounted for less thatn 20% at various levels. Depositional growth accounted for 56% at 8 km, and became the main mode at 5-8 km. Differently, droplet accretion of snow was important at levels below 5 km where existing relatively large amount of cloud water, accounting for 75-80% of total mass source. Therefore, the riming process was responsible for accumulation of snow at levels just above the 0^{o}C layer

According to observations and model results, cold rain precipitation was the primary mechanism. By calculating instantaneous precipitation rates at the bottom of the ice layer, the mixed phase layer and the warm layer, we found their contribution to precipitation mass were 10-20 %、50-65 %, 20-35 %, respectively. The contribution of the mixed phase layer varied corresponding to updrafts and liquid water content.

4. Conclusions

Based on airborne observations and surface facilities, the cloud structure and precipitation processes were studied comprehensively with the Weather Research and Forecasting (WRF) model.

The cloud development can be characterized by cirrus clouds at the initialization phase, upper cirrus, middle altostratus and lower stratocumulus clouds at the mature phase, and altostratus and stratocumulus clouds at the dissipating phase. Both radar measurements and model results suggested that embedded convective cells were present at the mature stage.

For the late mature stage, particle concentrations at 3.6 km decreased more evidently, with large particle concentration decreased to only 10^{1} L^{-1} and LWC to less than 0.001 g m^{-3}. That indicated rapid dissipation of lower stratocumulus clouds.

Snow was the primary precipitation particles in the cold layer, with the maximum content of 1.0 g m^{-3} and concentration of around 20 L^{-1}. Model results suggested that depositional growth accounted for 50 to 80 % of total snow growth for the levels above 6.0 km, while riming replaced depositional growth as the main mode below 6.0 km. Besides, due to thin warm layer, melted ice particles accounted for up to 70-90 % of raindrop source and gravitational coalescence only 10 %.

In the mature phase, the contribution of the ice layer decreased to 10 %, while the mixed phase layer and warm layer increased to 65-70 % and 20-25 %. Updrafts, supercooled water content and the top height of supercooled water were key factors affecting gowth of snow and subsequent precipitation rates.

Acknowledgements

Support was provided by the Key

Projects of the Ministry of Science and Technology of China (Grant 2006BAC12B00-01-06) and the Beijing's Key Discipline (Atmospheric Physics and Environment) Sponsoring Project.

References

Hobbs et al., 1975; Herzegh and Hobbs, 1980; Lo and Passarelli, 1982; Field, 1999; Field and Heymsfield, 2003; Heymsfield et al., 2008

Hobbs, P.V., 1975. The Nature of Winter Clouds and Precipitation in the Cascade Mountains and their Modification by Artificial Seeding. Part I: Natural Conditions. J. Appl. Meteor. 14, 783-804.

Herzegh, P.H., Hobbs, P.V., 1980. The Mesoscale and Microscale Structure and Organization of Clouds and Precipitation in Midlatitude Cyclones. II: Warm-Frontal Clouds. J. Atmos. Sci. 37, 597-611.

Lo, K.K., Passarelli, R.E., 1982. The Growth of Snow in Winter Storms: An Airborne Observational Study. J. Atmos. Sci. 39, 697-706.

Field, P.R., 1999. Aircraft observations of ice crystal evolution in an altostratus cloud. J. Atmos. Sci. 56, 1925-1941.

Field, P.R., Heymsfield, A.J., 2003. Aggregation and Scaling of Ice Crystal Size Distributions. J. Atmos. Sci., 60: 544-560.

Heymsfield, A.J., Field, P., Bansemer, A., 2008. Exponential Size Distributions for Snow. J. Atmos. Sci. 65, 4017-4031.